Measurement: Sensors 23 (2022) 100410

Contents lists available at ScienceDirect

Measurement: Sensors

journal homepage: www.sciencedirect.com/journal/measurement-sensors

Investigations on the potential application of machine vision lenses for depth measurement by exploiting chromatic aberrations

Robin Horn [a,*], Maik Rosenberger [a], Andrei Golomoz [a], Richard Fütterer [a], Paul-Gerald Dittrich [a], Rico Nestler [a], Gunther Notni [a,b]

[a] Technische Universität Ilmenau, Department of Mechanical Engineering, Group for Quality Assurance and Industrial Image Processing, Ilmenau, Germany
[b] Fraunhofer Institute for Applied Optics and Precision Engineering, Jena, Germany

ARTICLE INFO

Keywords:
Chromatic aberrations
3D depth reconstruction
Image processing
Multispectral imaging
Focal shift

ABSTRACT

Chromatic (spectral) aberrations are image imperfections that are disadvantageous for standard image processing tasks and are typically compensated through the application of different types of glass during lens design. The longitudinal chromatic aberration causes a relative unsharpness over different spectral channels. Since this error is corrected in most multi-chromatic lenses, this paper investigates to which extent the shift of the focal planes in a standard lens can be used specifically for image processing applications. Theoretical investigations of the longitudinal chromatic aberration are carried out. Based on this, conditions and a method to generate a 3D depth reconstruction out of different spectral channels are presented.

1. Introduction

This work is an extension of the paper entitled: "Investigation on chromatic aberrations and its potential for application in depth measurement" [1] and is based on the fundamentals of this previous research. In addition to the preceding basic investigations, further examinations of the depth measurement from the longitudinal chromatic aberration on lenses are carried out. The remaining topics of the fundamental work are continued and expanded by these investigations.

Optical systems consisting of one or more lenses are characterized by aberrations. The primary purpose of optical design and thus the preliminary work for camera lenses, vision and imaging systems is the fundamental reduction or even elimination of optical aberrations. This is achieved by an interplay of different lens designs consisting of a wide variety of optical materials.

Lenses are usually optimized to a certain point where only some errors are present to a sufficiently small degree. Only if an optic is almost perfectly free of aberrations it is suitable for precision optical measurement tasks.

Here we present the approach to use aberrations to realize certain optical measurement tasks. The chromatic aberration of the longitudinal error causes an axial offset of the wavelength dependent focal point [2]. Thus, it would be possible with a fixed sensor plane and different reference wavelengths to obtain sharp images of certain object distances. Depending on the object position, these focal planes can be shifted to the sensor and therefore a certain distance range of the object can be resolved and measured.

In this paper it will be initially determined whether with a simple lens and a wavelength selection the effect of longitudinal chromatic aberration is present to an appropriate degree in order to subsequently perform length measurements in the object space with the evaluation of the sensor image. From the processed data, a 3D depth representation, i. e. the depth information of an object by means of passing through the chromatic areas, can be created.

Subsequently, based on these results, a similar method of measurement is applied to a complex lens. Here, the previous numerical model cannot be applied. For this purpose, first of all a preliminary analysis is presented, which defines the properties of a lens for such an optical measurement. Based on this, a reference lens is measured using identical measurement conditions. The achievable measurement accuracy of the lens is presented and an assessment of the applicability of such an optical measurement method is provided.

2. Physical approach for the estimation of chromatic focal shift for depth measuring application

The longitudinal chromatic aberration is caused due to the dependence of the refractive index on the wavelength. In order to exploit this

* Corresponding author.
E-mail address: robin.horn@tu-ilmenau.de (R. Horn).

https://doi.org/10.1016/j.measen.2022.100410
Received 30 March 2022; Accepted 4 August 2022
Available online 17 August 2022

error for a depth measurement, it is important to understand how it occurs. It is best explained using a single bi-convex lens. In the field of geometrical optics, it can be assumed that a polychromatic and axis-parallel beam which runs outside the optical axis is chromatically split after passing through the lens and the individual wavelengths are refracted differently.

This collimated polychromatic light beam will experience different focal points in its spectral range. The focal length f(λ) increases with wavelength i.e. blue light has a shorter focal length than red light. The measurable distance of the focal points is also described as axial chromatic aberration [1].

$$D(\lambda) = \frac{1}{f(\lambda)} = (n(\lambda) - 1)\left(\frac{1}{R_1} - \frac{1}{R_2}\right) \tag{1}$$

Equation (1) the lens maker's formula describes the refracting power D(λ) of the lens. It is calculated with the wavelength dependent refractive index n(λ) and with the radii of curvature R_1/R_2 of the lens surfaces. The reciprocal of the refracting power is the effective focal length f(λ) which is needed to determine the focal point shift [3].

Fig. 1 explains the object distance shift in the field of geometrical optics. The upper drawing shows how the rear focal points and the image distance are affected by different wavelengths of a fixed object distance. The lower drawing takes the new wavelength depending focal points and displays the occurring object distance offset if the image plane stays in place and the wavelength changes. This effect is the focal point shift caused by the longitudinal chromatic aberration.

To calculate an object distance g(λ) with the help of the focal point shift, the lens equation (2) (imaging equation) is used. By rearranging (2), the wavelength-dependent object distance of a lens can be determined (3). If (1) is now substituted into (3), an equation (4) is obtained which describes the object distance only as a function of the wavelength-dependent refractive index. The remaining parameters are given by the lens properties and the selected image distance b and are therefore constant in the equation. To calculate the offset of the object distance Δg (λ), a zero point is determined for the first object distance at an initial wavelength of $\lambda_0 = 330$ nm. The difference for the subsequent values is defined according to (5) over a specific wavelength range (λ_n). The object distance offset corresponds directly to the desired depth information of an image to be measured.

$$\frac{1}{f(\lambda)} = \frac{1}{g} + \frac{1}{b} \tag{2}$$

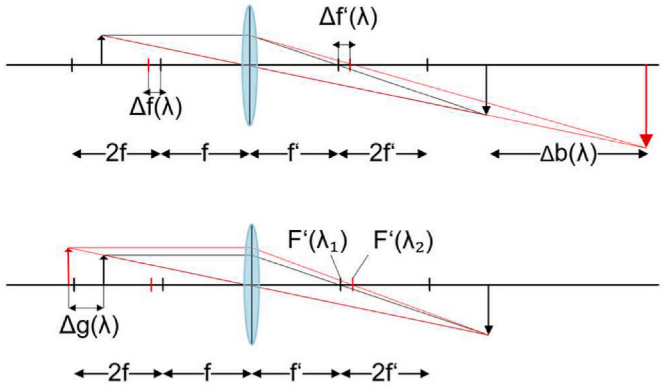

Fig. 1. Focal length depending on object distance.

$$\frac{1}{g(\lambda)} = \frac{1}{f(\lambda)} - \frac{1}{b} \tag{3}$$

$$g(\lambda) = \frac{R_2 R_1 b}{((R_2 - R_1)(n(\lambda) - 1))b - (R_2 R_1)} \tag{4}$$

$$\Delta g(\lambda) = g(\lambda_n) - g(\lambda_0) \tag{5}$$

It is now assumed that the imaging takes place at twice the focal length (magnification factor of 1). A single bi-convex lens made of N-BK7, with a focal length of 50 mm will therefore have an image distance of 100 mm. Fig. 2 displays the offset of the object distance and the refractive index both dependent on the wavelengths for the depicted lens [4].

In order to estimate how significant, the error caused by a real lens is and to verify the calculated object distance offset, simulation models are created with the help of Zemax-OpticStudio ® [5]. A single bi-convex lens with the same parameters which have been used in the calculation is evaluated. Later a comparison will be made by experimental tests with the finished experimental setup of a multispectral image acquisition system.

3. Numeric model to assess the chromatic focal shift

Based on the numerical model of the single bi-convex lens, it is impossible to form a general model for a more complex lens system. There are several reasons for this. Since lenses are designed for special tasks, the design data for them are usually not available to the public. Since an available example lens was used for the following considerations, it was not possible to access the design data in order to gain a closer insight into the specific design and the types of optical materials used. A basic consideration of the known and relevant lens parameters will be carried out.

A lens can either have a fixed or variable focal length (by shifting individual lens assemblies). Equations (4) and (5) may be applied in the same manner as for the single bi-convex lens. It is not possible for a mere theoretical consideration since the principal planes of the lens cannot be determined without having knowledge of the design of the lens.

From this fact no unambiguous numerical assignment of the image and object distance can be generated here. A numerical consideration on the basis of the lens equation is thus impossible.

Also, no conclusion can be drawn to an effective refractive index of the system. It is not possible for the example lens used here to characterize the glass types and thus the refractive indices of the individual lenses which have a direct influence on the focal shift of the lens [6]. Thus, it is not possible to calculate the wavelength-dependent object

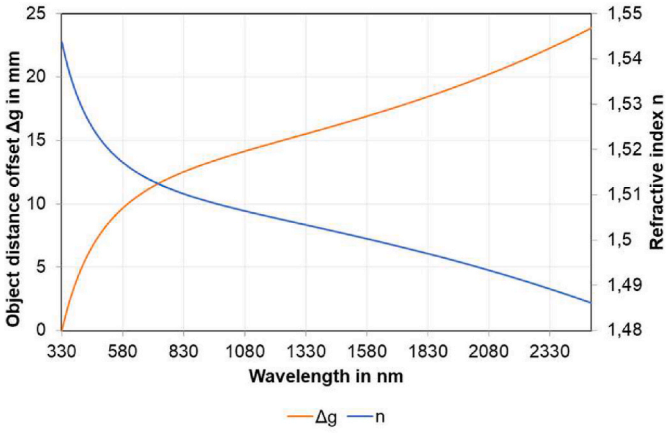

Fig. 2. Offset of the object distance and refractive index dependent on the wavelengths.

distance and thus the depth information. It is well known that lenses are optimized within the spectrum of their application wavelengths. This means that for a specific wavelength range, aberrations, including chromatic aberration, are not present or are so minor that they are not detectable. The optimized optical system simultaneously corrects other aberrations that are not further discussed [7,8].

The correction of chromatic aberrations is achieved by using achromats. An achromatic lens pair enables a compensation of the focus shifts of the edge bands for the corrected wavelength range due to the composition of the lenses (respectively high and low refractive index glass types). Here, the range of blur and thus the so-called circle of confusion can be reduced by a significant factor compared to a single lens [9–11]. Since lenses are composed of such achromatic systems, a similar reduction of the effect can be assumed for them.

This general optimization is disadvantageous for the application intended here, which is to use the longitudinal chromatic aberration for 3D depth measurements. Fig. 3 shows the corrected longitudinal aberration and the focal shift of an example lens. Lenses are usually corrected in the visible wavelength range around 550 nm, since this is where most standard image processing is performed. However, special lenses can also be optimized for the infrared spectral range or the ultraviolet range [12].

Here it can be observed that for a center wavelength and the surrounding area the chromatic aberration has a very small impact. However, if one observes, for example, higher wavelengths, the influence of the chromatic aberration becomes significantly more distinct. In the range from 600 nm to 1000 nm, the focal shift increases almost linearly.

This condition shows that despite the corrected aberrations, a residual error for non-applicable spectral ranges is present and can be exploited.

The specific known data, which are commonly available for a lens and which are important for the determination of the spectral dependent focal shift, are the effective focal length of the optical system and the f-number or aperture. It is noted at this point that the equations of section 2 can be applied in the main statement for a more complex system than a single lens. However, since the effect for an actually corrected system is significantly reduced, further parameters are added to the theoretical consideration. These parameters are the aperture and the depth of field (DOF). Without being able to make any specific conclusions about a lens design, these parameters play an important part in determining the focal shift caused by chromatic aberration.

Consequently, the focal shift in an uncorrected wavelength range is assumed to behave the same as that of a single lens. However, since the effect is corrected in a certain spectral range, the consideration of focal length, depth of field and aperture becomes crucial. Since no specific information is available on the composition of the lens, a review of these lens parameters is presented in this section. These parameters are

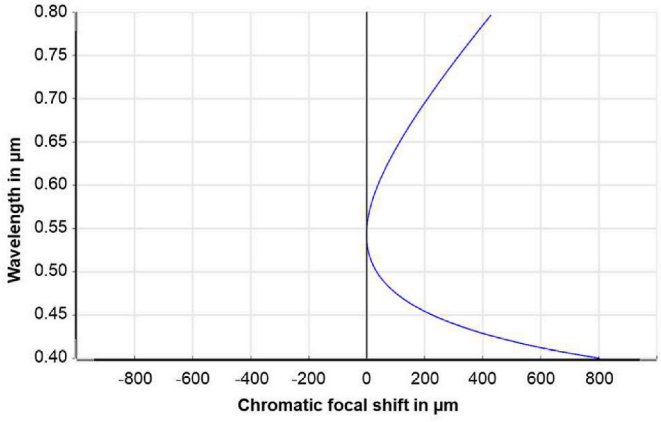

Fig. 3. Chromatic focal shift of an example lens.

connected with each other and have a further influence on the measurability and the applicability for a 3D depth measurement exploiting the longitudinal chromatic aberration.

The most critical parameter is the depth of field of the lens for determining the shifted focal planes and therefore different image sharpness [13]. Machine vision lenses are usually designed with a relatively large depth of field, allowing various objects of interest to be imaged sharply within the area of interest. However, this effect of a large depth of field is disadvantageous for a measurement with the chromatic focal shift. This means that if the depth of field area is significantly larger than the range of the focal shift, the chromatic focal shift simply cannot be determined. It should be noted that the focal shift, as calculated by equation (5) according to the principles of geometric optics, is dependent on the focal length, the aperture and the circle of confusion (whereby these parameters have an influence on the depth of field) as well as the object distance g [14,15].

$$DOF(\lambda) = g_{far}(\lambda) - g_{near}(\lambda)$$

$$DOF(\lambda) = \frac{g(\lambda) f(\lambda) \frac{f(\lambda)}{N}}{f(\lambda)\frac{f(\lambda)}{N} + g(\lambda)c} - \frac{g(\lambda) f(\lambda) \frac{f(\lambda)}{N}}{f(\lambda)\frac{f(\lambda)}{N} - g(\lambda)c} \tag{6}$$

The depth of field results from the distances from the near and far points of the object widths at which the object point can still be sharply imaged in terms of the maximal diameter of the circle of confusion (Equation (6)). Since these two distances are dependent on the focal length f, this effect is also dependent on the wavelength λ used.

The circle of confusion c is not defined here with a specific value, however, it can be noted here that for a sharp representation of the image point the circle of confusion should typically have the diameter of 2 pixels of the sensor used, because the image sharpness is described by the diameter of the circle of confusion [16,17].

The f-number N, which affects the depth of field, also depends on the focal length and the diameter of the aperture stop D, and thus on the effective aperture of the system. The aperture of the optical system describes how much light can be absorbed by the system. The expression $N = f/D$ describes therefore the f-number [18].

A numerical determination of the respective parameters in dependence of the wavelength and the resulting variable focal length is not possible without knowing specific data of a lens. However, a qualitative statement can be made as to how these parameters have to be combined in order to generate a minimal depth-of-field range and thus to be able to generate depth information from the longitudinal chromatic aberration by shifting the object distance. This means that the smallest possible depth-of-field range is generated by using a small focal length and a large aperture, i.e. a minimum f-number.

In conclusion, without the knowledge of the specific design of a lens it is not possible to create a numerical model to describe the wavelength dependent focal shift. However, the further considerations show that by maintaining certain parameters and performing a measurement in the non-corrected wavelength range of the lens, it should theoretically be possible to use the originally compensated chromatic aberration for a 3D depth measurement.

4. Method for determining the 3D depth information

The numerically calculated object distances of an image can be converted to 3D depth information by (5) as described in section 2. For the verification of a real system, consisting of the single bi-convex lens, a possibility is now introduced to convert the length information from the object distance into depth information with the help of a subsequent image processing.

For this purpose, a Matlab ® [19] program was developed, which calculates and transforms focus information from 2D images into a 3D image. Fig. 4 describes the basic operation of the program.

To perform such an evaluation, it is necessary to record a series of

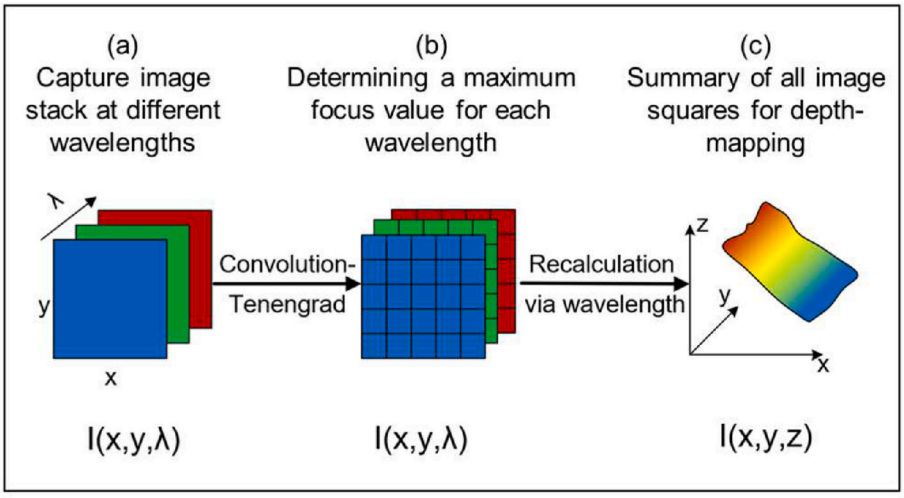

Fig. 4. Schematic course of image processing for the determination of depth information using only wavelength information.

images in the desired wavelength range. By modulating a light source, a spectrum with 1 nm bandwidth can be provided for each individual image ((a), Fig. 4). According to the numerical approach, different object distances are also expected to have different focal planes. Each image therefore has a corresponding object distance for its wavelength. A loop is applied in which a parameterized mask is placed over the images as a square grid ((b), Fig. 4). For each square in the grid, a focus value is determined using a sharpness operator. The operator used here is the Tenengrad-Gradient (7) which convolutes the image with 3 × 3-Sobel-Operands s_x and s_y in both x and y orientations [20].

$$S = \sum_{(x,y)\in I} \left(I(x,y)*s_x\right)^2 + \left(I(x,y)*s_y\right)^2$$

$$s_x = \begin{bmatrix} -1 & 0 & 1 \\ -2 & 0 & 2 \\ -1 & 0 & 1 \end{bmatrix};\ s_y = \begin{bmatrix} 1 & 2 & 1 \\ 0 & 0 & 0 \\ -1 & -2 & -1 \end{bmatrix} \tag{7}$$

These steps are repeated for the entire image stack. The focus values are then compared for each square in the grid. The maximum values for the respective image area are assembled as a new image ((c), Fig. 4). The newly composed image now consists of the sharpest planes of the individual wavelengths. Using the computation formula (4) and (5), depth information can now be obtained from the image. The last step is a surface plot which maps the depth information as a 3D depth representation. These steps are sufficient for the measurement using the single bi-convex lens, since the theoretical model of the displacement of the object distances serves as a basis for the calculation. However, since the model presented in section 3 cannot be directly applied to a complex lens, it is necessary to develop an extension of the algorithm, which is capable of determining the existing object displacement by means of an inverse calculation on the basis of a calibration object. Using the procedure described above again, allows a subsequently representation of 3D depth information of an unknown test object.

5. Experimental generation of 3D depth information

In the following section, the experimental results are presented for a single bi-convex lens and then for a complex lens. In addition, the more comprehensive process of generating a 3D image using a complex lens is presented in more detail with regard to the calibration process and the generated measurement output. The achieved resolution with the used complex lens is then described in more detail.

5.1. Verification of the numeric approach (single bi-convex lens)

The numerically determined values of the single bi-convex lens are now being verified by means of an image evaluation. For this purpose, the image processing program which determines the focus values of individual image sections and compares them over their individual wavelengths, like described in section 4, is used.

The same type of single bi-convex lens as in the previous simulation was used to realize a test setup.

It consists of a multispectral light source and the lens used as an objective for a standard 2D sensor. Fig. 5 presents a schematic realization of the test setup. For a better visualization, an arbitrary test object is used here.

Single spectra of 1 nm bandwidth are generated with the help of a modulable light source. An inclined plane was used as a test object. This was aligned in such a way that its depth information can be sufficiently represented over the sensor surface. This means in a 45° angle to the sensor surface. With the given dimension and a magnification factor of 1, a depth of 6 mm could be displayed. The intension is to confirm the numerical and simulated values of the focal shift. Additionally, this allows a first estimation in which measurement-range it should be possible to acquire useful measurement results with a complex lens. Since the depth information of the test object is known by the position of it, it is possible to obtain conclusions about the correctness of the measured values. Since the technical equipment does not allow a complete evaluation of the entire visible wavelength range, tests haven been performed in a wavelength range from 500 nm to 600 nm. For this purpose, as mentioned above, 101 images have been acquired and evaluated in 1 nm steps. The result is shown in Fig. 6 and compared again with the numerical data in Table 1.

To compare the experimental data with the numerical ones, the geometric course of the inclined plane has to be defined. The measurable real depth of the plane can be determined with (8). This can be used because the mapping is performed with a magnification factor of 1.

$$Depth\ inclined\ plane = \frac{Image\ height}{\tan(\alpha)},\ \alpha = 45° \tag{8}$$

The lower edge of the image area corresponds to a depth of 0 mm because the image height is zero. For each image height, a depth can be calculated, which are both equal. This is justified because tan (45°) is equal to 1. In order to avoid further aberrations, like for example distortions, the effective measuring range was shifted to the centre of the image. The lower and upper flat areas in Fig. 6 show blurred planes. Due to the wavelength limitation, no reliable focus values could be determined at these locations. However, these errors do not affect the depth

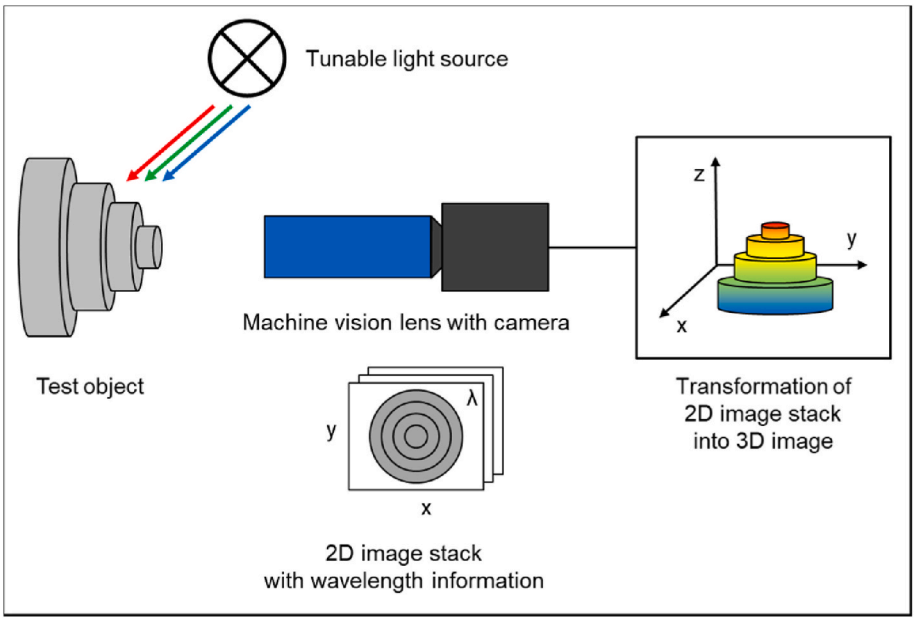

Fig. 5. Schematic representation of the test setup.

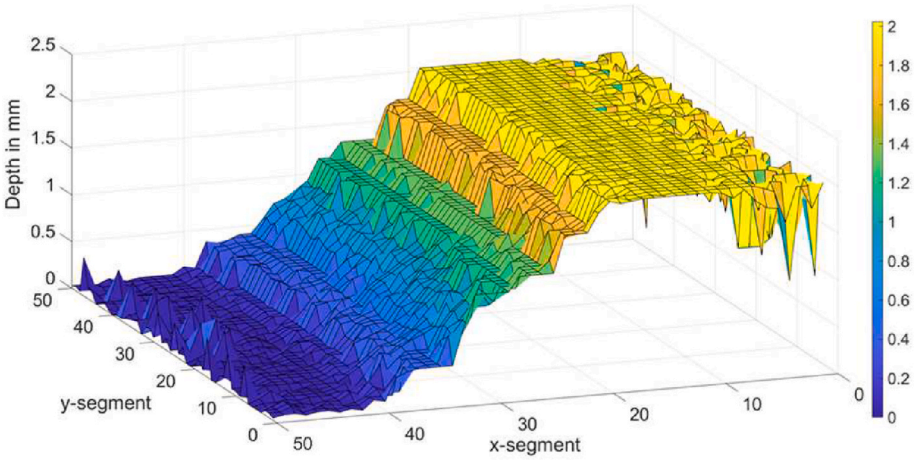

Fig. 6. 3D-map of test object (inclined plane).

Table 1
Comparison of the experimental data and the simulated/numerical data.

Wavelength in nm	Depth in mm	
	Experimental depth of inclined plane	Numeric/Simulated
500	0 (shifted)	0
520	0.636	0.487
540	1.116	0.928
560	1.696	1.328
580	2.014	1.692
600	2.120	2.025

determination in the measurement area. The zero point for calculating the position of the inclined plane is therefore simply shifted in the image height to match the initial wavelength at 500 nm. In this way, reliable values can be obtained for the measurement range.

In Table 1, the experimentally determined depth and the numerical data are compared. The depth of the inclined plane is shown for the respective point at which the associated wavelength is most significant. For the single bi-convex lens the experimental data are approximately the same as the numerical for the respective wavelength.

The small deviation between the simulated depth of the plane and the experimental data can be explained by the angular error and stems from the simplified calculation. A high-precision alignment of the angle of the inclined plane in the arc-second range could not be achieved, resulting in a small deviation based on the angular offset. This is because the image of the depth information represents the real system. This means that the error resides in (8) and not in the experimental data.

5.2. *Evaluation of the attainable 3D depth information based on a complex lens*

Following the successful measurements on a single bi-convex lens, an extended measurement setup was realized. By increasing the available spectral range through the use of a monochromator [21], it was also possible to measure beyond 600 nm evaluating the lens. By using the monochromator, it is possible to measure the object in the required spectral range from 550 nm to 1000 nm with a precise bandwidth of 1 nm.

In order to homogeneously illuminate any three-dimensional measuring object, a diffuser was used in front of the light source and

the illumination was arranged in such a way that the object is illuminated almost perpendicularly.

The lens used here is a macro-lens with variable focal length and aperture. Depending on the requirements described in section 3, these parameters were set to achieve the narrowest possible depth of field at the shortest object distance. Table 2 summarizes the relevant parameters of the experimental setup and the lens.

An initial measurement was performed in bigger wavelength steps ($\lambda = 50$ nm) to determine when a change in focus due to the wavelength becomes apparent. It can be seen that after an assumed central wavelength of around 550 nm, a clear focal plane shift becomes detectable with increasing wavelength. Therefore, individual images have been generated with a bandwidth of 1 nm in a wavelength range from 550 nm to 1000 nm in steps of 5 nm. To enable a focus determination for a large wavelength range, an identical gray value distribution is set for each image in a selected image area. For this purpose, an average gray value of 140 was determined for the 8-bit CCD camera with the sensor Sony ICX424 which was used. The exposure time is adjusted for each individual image so that the generated images can be calculated using the same procedure applying a focus criterion. First, an inclined plane was examined in the same way as the single bi-convex lens approach. This inclined plane acts as a calibration object to determine the range of the focal shift, the meaning of which will be described in more detail in the following.

5.2.1. Calibration of the 3D depth information

A special characteristic of the more complex setup, is that due to an insufficient knowledge of the lens, a numeric method for the wavelength-dependent change of the focal plane and consequently of the object distance cannot be applied. This implies that the inclined plane cannot directly be quantified in different monochromatic wavelengths and subsequently a depth information cannot be obtained straight from this measurement. The measurement described in the following allows a calibration of the complex lens and its parameters through a specific algorithm. Similar to the method used in section 5 with equation (8) to obtain the depth of the inclined plane, trigonometric equations are used here. Thus, with the known angle of the inclined plane α and the hypotenuse of this plane s which is in focus over the measuring range, a in focus depth range DOF_{range} can be calculated.

From this range, a factor m can be calculated by equation (10), which allows to calculate a depth in connection with the associated wavelength.

$$DOF_{range} = s \cdot \sin(\alpha)\ ,\ \alpha = 56,3^{\circ} \tag{9}$$

$$m = \frac{DOF_{range}}{Wavelength\ range} \tag{10}$$

$$Depth_{measurement} = \lambda_n \cdot m \tag{11}$$

The application of these equations allows to draw a conclusion which object distance is imaged sharpest under the corresponding wavelength illumination. For this process, an extension of the algorithm described in section 4 is used here. By performing these additional calculations (equations (9) to (11)), a parameter m can thus be determined which defines the dependence of the wavelength on the measurable depth. A significant simplification can be used by assuming that the lens has a linear dependence of the focal shift and the object distance in its uncorrected wavelength range, especially in the measuring range used here. The linear relation in equation (10) can be applied, since Fig. 7 can be approximated by a linear function. Here it can be clearly seen that the focal shift is gradual shifted over a *wavelength range* from 550 nm to 1000 nm, but also linear over an image area of about 368 pixels. Whereby the image space can be converted simply by the pixel size and the image scale into a length in the object space.

A threshold condition locates the sharpest image area of the composite image and assigns it to the corresponding wavelength. The inclined plane was provided with a scale for this purpose. Fig. 8 (a) and (b) shows the inclined plane which contains different scales in 10 mm increments of the large areas and 0.625 mm for a black to white increment. Likewise, the limits of the shifted depth of field can be determined for the acquired image stack. Within this shifted depth of field range, it is possible to measure the longitudinal chromatic aberration.

Using the known depth of the scale (which represents the hypotenuse in the image), the achievable maximum depth for a 3D conversion of the focal shift can thus be determined. Fig. 8(c) shows the start and end range of the shifted focus area.

Since the calculated factor m can be easily compared with the known actual depth values of the inclined plane, it can be verified as to its accuracy. Also, a correction of the parameter becomes possible which allows a generation of more precise results at the measurement of unknown objects. Since by this calculation a first assignment of the wavelengths to an object offset is possible, on basis of the program described in section 4 a 3D reconstruction can be generated.

5.2.2. 3D depth information generation using a reference object

Since a calibration algorithm is now available to link the object distance offset to a wavelength, it is possible to measure an "unknown" object. Fig. 9 displays the measurement object. This measurement object had to be additionally modified to have approximately the same spectral properties on the high bandwidth of the measurement spectrum. In addition, the surface needs to have a distinct texture in order to be distinguishable for the applied sharpness criterion in the evaluation. Since a flat surface without structure cannot be differentiated between focused and blurred.

The test object also has an inclined plane at an angle of 50°. This inclined plane is necessary for the investigation of the achievable measurement resolution.

The measurement with this test object was performed in the same wavelength range as the calibration object. That means in the range from 550 nm to 1000 nm with 1 nm bandwidth in 5 nm steps so 91 images have been captured. Using the program described in section 4, a

Table 2
Parameters of the lens used in the setup.

Lens parameters	Value
Focal length	35 mm
F-number	2.8
Depth of field (measured)	6.8 mm
Multichromatic object distance	178 mm
Magnification	1:6.75

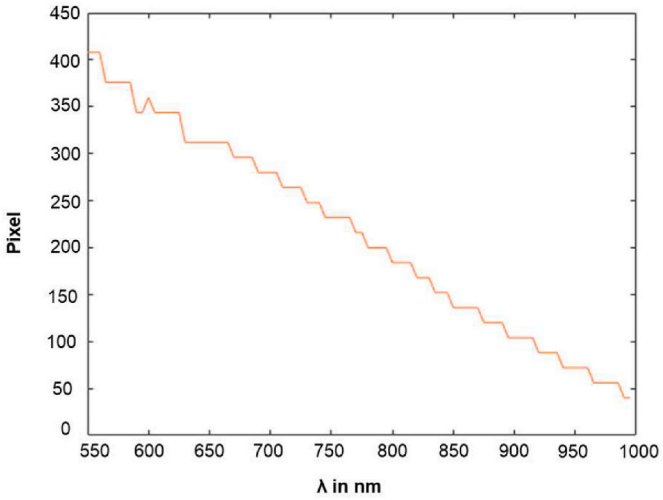

Fig. 7. Sharpest image area (pixel) depending on the wavelength lambda.

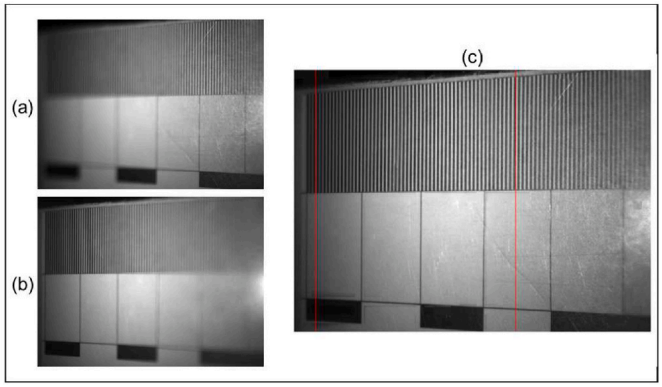

Fig. 8. DOF at the start-wavelength of 550 nm (a) and at the end-wavelength of 1000 nm (b) and the full depth of field range over the measurable wavelength range marked by the red lines (c) 33.125 mm as hypotenuse and 18.4 mm as measurable depth. (For interpretation of the references to colour in this figure, the reader is referred to the Web version of this article.)

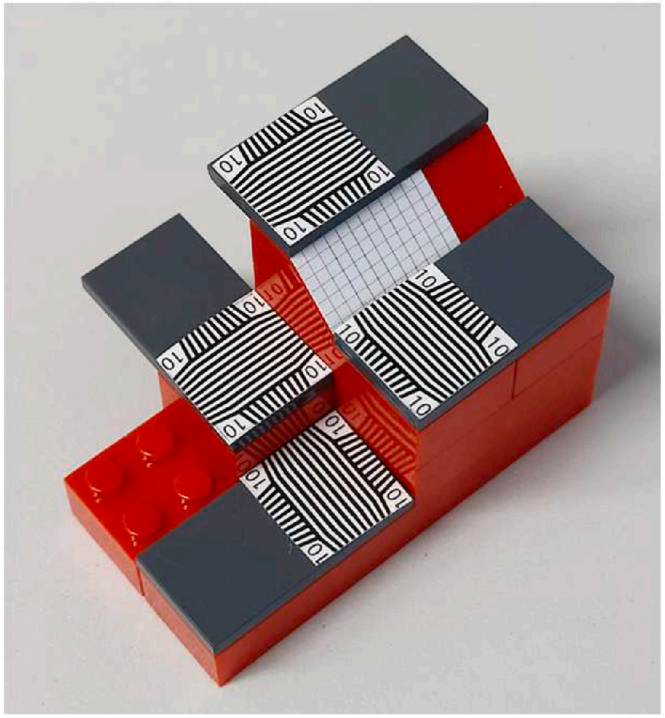

Fig. 9. Test object with depth information.

reconstructed image, Fig. 10, of the test object could be generated.

The areas of the planes are composed of about two to three wavelengths. This effect can be explained by the depth of field range, because for multiple wavelengths, several pixels on the respective plane are arbitrarily displayed in focus.

If this reconstructed image is transferred to the 3D representation shown in Fig. 11, it becomes apparent that, although the height and depth information of the object can be recognized, distinct image imperfections are present.

These imperfections are due to the fact that several wavelengths come into consideration for the sharpest pixel areas. This issue arises from the extended depth-of-field range of multiple wavelengths and thus focal planes of the same or similar sharpness contributing to the image. This effect could be improved by reducing the depth of field. Also, the calibration of the wavelength to the given object distances causes a specific uncertainty in the measurement results of a plane. Again, this is

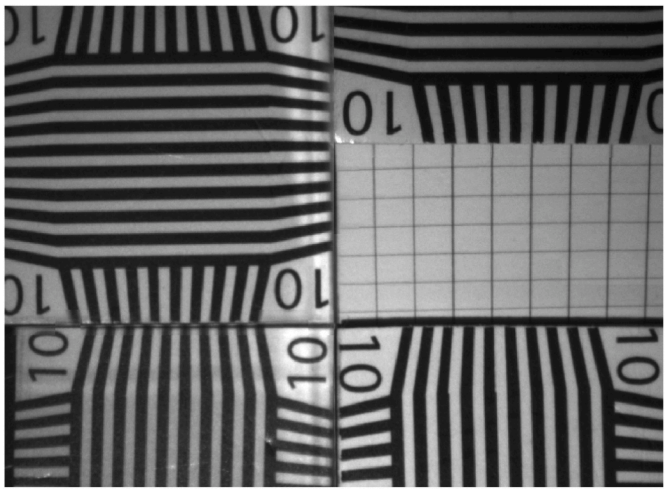

Fig. 10. Reconstructed sharp image of the test object.

due to the ambiguity of the image segments with respect to their sharpness and the assigned wavelength and consequently the object distances.

Table 3 shows the distances in the form of the measurable depth of the four surfaces, if the uppermost surface (the surface with the shortest object distance from the lens) is represented as reference surface at a depth of 0 mm. It is important to note that the surfaces orientations are inverted for the 3D representation. Here, a specific wavelength range can be defined, which can be assigned to a measurable depth especially for the lens used here. The deviation of the experimental data from the real depths of the object can be associated on the one hand with the approximation of the linearity of the focal shift and on the other hand with the general generation of the approximated depth values depending on the assignment of a specific wavelength from the calibration process.

Despite a distinct difference of about 2 mm of the measurement data from the real depth of the object, it can be concluded that a systematic error is present. Regardless of the deviation of the measurement results, the conclusion can be made that an application of such a measurement setup, using only the chromatic aberration for the measurement of depths and the generation of 3D depth information is possible.

5.2.3. *System resolution*

From the measured values achieved in Fig. 11, particular uncertainties and errors can be identified for the deviation of the measured data from the real depth values. These errors can be attributed to specific characteristics of the process of the data generation used here. On the one hand, the focal shift of the individual wavelengths is determined on the basis of a calibration object. Here, ambiguities for the focal shift and the associated wavelength can already occur in this process. In addition, the course of the focal shift and thus the object width change was assumed to be linear, which cannot be unambiguously proven for the lens used. Although all parameters described in section 3 are set to reduce the depth of field range, this effect is still present to an extent that an incorrect assignment of several wavelengths to a defined object distance occurs.

Despite the lack of essential parameters, a 3D reconstruction of the depth information of an unknown measurement object could be created. For this purpose, a qualitative determination of the measurement resolution was made for the test lens used. Since a total depth of 26.6 mm could be measured within a wavelength range of 450 nm, it is possible to estimate the achievable measurement resolution additionally considering the inclined plane.

The inclined plane has been represented by 26 wavelengths steps, that corresponds to a wavelength range of 130 nm. The analysis of the

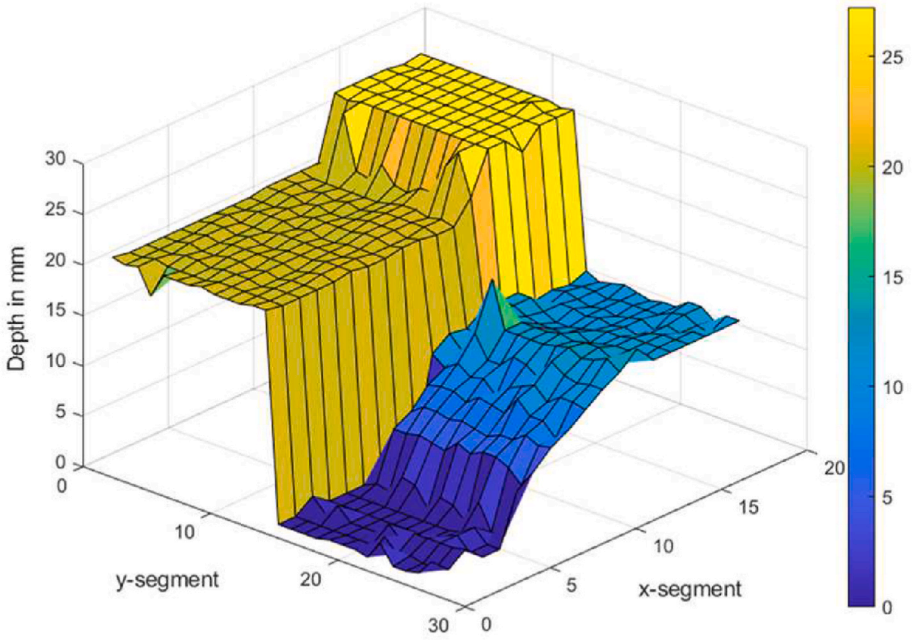

Fig. 11. 3D-representation of the test object.

Table 3
Measurement data – 3D depth information test object.

Surface	Depth in mm	
	Experimental depth of test object	Real depth
1	0 (shifted)	0
2	11.5	9.5
3	20.5	19
4	26.6	28.5

inclined plane shows that for each image area a difference of 3 wavelength steps is not distinguishable for the determination of the image sharpness. This implies that only steps of 15 nm difference are resolvable. This yields a resolution of about 1.1 mm per distinguishable area, i.e. per 15 nm. This measurement uncertainty also accounts for the uncertainty in the 3D representation, since here a specific wavelength is assigned to exactly one distance. The resolution of 1.1 mm/15 nm describes the maximum achievable effective resolution for the used lens in the test setup.

A potential theoretical measurement resolution can be obtained assuming 'perfect' parameters from section 3. The theoretical resolution can be improved to 0.073 mm per single nanometer. This implies that the depth-of-field range needs to be less than this resolution limit. One way to achieve this, is to allow significantly larger aperture. However, it should be noted that a significant improvement of the resolution achieved here is possible for enhanced setups.

6. Conclusion

The initial investigations of a single bi-convex lens showed that it is possible to produce reliable 3D images from different spectral channels by exploiting the longitudinal chromatic aberration. Based on these insights, it was investigated if it is possible to generate equivalent measurement data with a complex lens. Since essential parameters are not available due to no disclosure of the lens design data, a systematic approach was discussed to exploit the longitudinal chromatic aberration for depth measurement regardless of the lack of lens characteristics. After determining the relevant and available parameters of the lens, such as focal length, aperture, and depth of field, an initial measurement could be made using a selected example lens. A successful representation of the depth information of a test object could be achieved by the exclusive exploitation of the longitudinal chromatic aberration. In addition, the achievable effective resolution was determined for the used lens. This resolution can be significantly improved by changing the lens parameters.

It can be seen here that an aberration-corrected lens does not provide a distinct improvement, i.e., a reduction in the measurement range and a significantly higher resolution than a single bi-convex lens. However, these qualities can be achieved by a significant reduction in the depth-of-field range, which is the most limiting factor. In summary, the potential application of lenses for such a measurement could be demonstrated without knowing explicit numerical information of the lens. It remains to be verified how far the effect can be exploited under knowledge of the lens design.

The knowledge obtained in this research indicates that an application of depth determination using this measurement method could be used as a general estimation of depth information. A machine vision lens provides enhanced 2D imaging properties due to its standard design. A simultaneous use of such a lens to generate 3D information is also possible according to the results presented herein.

If this first proof-of-concept is further optimized, a measurement of the spectral properties of an object can also be performed using suitable light sources, since a certain spectral range has to be covered for the effect of the focal shift to come apparent. A possibility for future application could be an extension of the concept introduced here to perform a simultaneous generation of information in 3-channels such as spectral, 2D and 3D, simply using a standard imaging system and an adequate evaluation algorithm.

Declaration of competing interest

The authors declare that they have no known competing financial interests or personal relationships that could have appeared to influence the work reported in this paper.

Acknowledgement

The first author would like to thank all co-authors for their support in

the execution of the measurement, the evaluation of the results and the preparation of the paper. The support by the Group for Quality Assurance and Industrial Image Processing of the TU Ilmenau, Germany, is gratefully acknowledged.

References

[1] R. Horn, M. Rosenberger, G. Notni, A. Golomoz, R. Fütterer, P.-G. Dittrich, Investigation on chromatic aberrations and its potential for application in depth measurement, Measurement: Sensors 18 (2021), 100113, https://doi.org/10.1016/j.measen.2021.100113.
[2] E. Hecht, Optics, third. ed., Addison-Wesley, Reading, Mass, 1998, p. 271.
[3] V.N. Mahajan, Optical Imaging and Aberrations: Ray Geometrical Optics, SPIE Press, Bellingham, Washington, 1998, pp. 25–26.
[4] Refractive Index of Schott N-BK7. Schott Optical Glass Catalogue of August 2010. https://www.filmetrics.de/refractive-index-database/Schott+N-BK7/, (accessed 24 February 2021).
[5] Zemax - OpticStudio. https://www.zemax.com/pages/opticstudio (accessed 01 February 2022).
[6] J. Zhuang, Q. Zhang, P. Wu, S. Han, Chromatic focal shift of optical system expressed by related wavelength formulas, in: Optical Modeling and System Alignment, SPIE, San Diego, United States, 2019, p. 7.
[7] M.J. Kidger, Fundamental Optical Design, SPIE, Bellingham, Washington, 2001, pp. 281–311.
[8] J. Shamir, Optical Systems and Processes, SPIE, Bellingham, USA, 1999, p. 122.
[9] V.N. Mahajan, Fundamentals of Geometrical Optics, SPIE, Bellingham, Washington, 2014, pp. 303–304.
[10] H. Haferkorn, Optik: physikalisch-technische Grundlagen und Anwendungen, Wiley-VCH, Weinheim, 2002, p. 653 (translated).
[11] B.H. Walker, Optical Engineering Fundamentals, second ed., SPIE, Bellingham, Washington, 2009, pp. 114–115.
[12] T. Acharya, A.K. Ray, Image Processing: Principles and Applications, John Wiley & Sons, 2005, p. 38.
[13] H.-C. Lee, Review of image-blur models in a photographic system using the principles of optics, Opt. Eng. 29 (1990) 406, https://doi.org/10.1117/12.55609 (405-421).
[14] J. Ens, P. Lawrence, An investigation of methods for determining depth from focus, IEEE Trans. Pattern Anal. Mach. Intell. 15 (1993) 97–99, https://doi.org/10.1109/34.192482 (97–108).
[15] R. Kosara, S. Miksch, H. Hauser, Semantic depth of field, in: IEEE Symposium on Information Visualization, 2001, p. 2.
[16] A. Miks, J. Novak, Dependence of camera lens induced radial distortion and circle of confusion on object position, Opt Laser. Technol. 44 (2012) 1047, https://doi.org/10.1016/j.optlastec.2011.10.012 (1043–1049).
[17] Vision Doctor. Depth of field. https://www.vision-doctor.com/en/optical-basics/depth-of-field.html. (accessed 16 February 2022).
[18] J. Bentley, C. Olson, Field Guide to Lens Design, SPIE, 2012, p. 4.
[19] MathWorks - Matlab. https://de.mathworks.com/products/matlab.html (accessed 01 February 2022).
[20] J.M. Tenenbaum, Accommodation in Computer Vision, PhD thesis, Stanford University, USA, 1970.
[21] Quantum Design Europe. Monochromator MSH-300. https://qd-europe.com/cz/en/product/msh-300-with-variable-slits-msh-300f-with-fixed-slits/(accessed 24 February 2022).